JOURNAL OF SPACECRAFT AND ROCKETS
Vol. 45, No. 3, May–June 2008

Space Event Detection Method

Russell P. Patera*
The Aerospace Corporation, Los Angeles, California 90009-2957

DOI: 10.2514/1.30348

A method was developed to detect space events, such as maneuvers, collisions, explosions, etc., involving space objects tracked by the Cheyenne Mountain Operations Center. The Cheyenne Mountain Operations Center creates state vector parameters for tracked objects and places them in a catalog with the corresponding time. This time dependent data can be processed to reveal sudden unexpected changes in parameter values referred to as space events. A moving window curve fit technique was found effective in estimating a parameter's value and detecting sudden changes indicative of space events. The moving window technique filters noise and permits processing of time varying data. When a parameter's deviation from its expected value exceeds a predefined threshold, an event is declared. The processing method was implemented and tested on space object data. Space vehicle maneuvers, collisions and space weather events were readily detected. The method does not involve state vector propagation and is very computationally efficient.

Nomenclature

c_i = polynomial coefficients of curve fit
E = total orbital energy per unit mass, m^2/s^2
G = gravitational constant, m^3/s^2
M = mass of the Earth, kg
n = mean motion (number orbital revolutions per day)
$p(t)$ = polynomial curve fit function

I. Introduction

IT IS increasingly important to be aware of space events such as space vehicle maneuvers, explosions, collisions, fragmentations, sudden changes in ballistic coefficients, solar corona mass ejections that impact the Earth, etc. For example, a severe solar event can affect all low Earth orbiting satellites [1]. Satellite operators need to be aware when such an event occurs so that mitigation action can be taken. An explosion could generate space debris that could cause collision risk to operational satellites [2,3]. Timely knowledge may allow mitigation measures to be taken. The importance of spacecraft maneuvers in the geosynchronous Earth orbit (GEO) altitude region led to recent research on GEO maneuver detection using a binary search method and an extended Kalman filter [4,5]. Unfortunately, a systematic means of detecting various kinds of space events based on orbital anomalies is currently not widely available.

This paper presents a data processing method that can be applied to an existing database of tracked space objects to detect space events. The input data to be processed is generated by the Cheyenne Mountain Operations Center (CMOC) and placed into a catalog of tracked objects [6]. The data are referred to as two-line element sets (TLEs) and consist of parameters needed to describe the orbits of tracked space objects. Each set of data has an associated time and six parameters that specify the respective orbit. The data processing method proposed here can be used on each parameter separately or it can be used on a parameters derived from one or more of the data set parameters.

Presented as Paper 6513 at the AIAA/AAS Astrodynamics Specialist Conference and Exhibit, Keystone, Colorado, 21–24 August 2006; received 8 February 2007; revision received 4 October 2007; accepted for publication 21 December 2007.

*Senior Engineering Specialist, Center for Orbital and Reentry Debris Studies, Mail Stop: M4-066.

This method is completely unrelated to the binary search method [4,5] of detecting spacecraft maneuvers, which searches for maneuvers by partitioning tracking data into segments that are found to contain no maneuvers via several goodness-of-fit criteria.

The processing method proposed in this work employs a moving window curve fit method akin to the moving average method used in statistical data processing. For each processing step, a single representative parameter value based on the polynomial curve fit is subtracted from the actual parameter having the corresponding time to obtain a deviation. The parameter deviation and associated time are saved. The saved deviations are then processed statistically to determine the mean, variance, and standard deviation. The event threshold is specified in units of standard deviation. Each deviation is checked to see if it exceeds the event threshold. If it does, an event is declared and the time and deviation are saved for future reference. The analyst can adjust the event threshold so that mostly events of interest are detected.

An alternative processing method can also be used. It involves finding the derivative of the fitted polynomial at the midpoint or other point within the data array window. The process proceeds as discussed earlier, only in this case, the parameter derivative replaces the parameter dispersion.

The moving window method serves to remove smaller variations due to orbital perturbations and noise while responding to slower secular variations in parameter values. In this manner, the larger deviations indicative of space events can be identified.

One can choose the threshold size to detect the range of events desired. Too small a threshold could result in too many less significant events. This could lead to an excessive amount of event analysis to determine the most significant events. It is preferable to choose a threshold small enough to detect events of interest, but not too many extraneous events.

II. Processing Scheme

Figure 1 illustrates the event processing scheme for the energy parameter. A description of each processing step in Fig. 1 is provided.

10: Sequential database for space objects has object number, time, and state vector parameters (eccentricity, mean motion, inclination, right ascension of ascending node, argument of perigee, mean anomaly) for each of the over 8000 tracked space objects.

12: Select sequential data for a single space object.

14: Energy is computed from the mean motion parameter for each set of sequential data.

16: A subset of sequential data is placed in the moving window data array. In this case, time and energy are placed in the moving window data array.

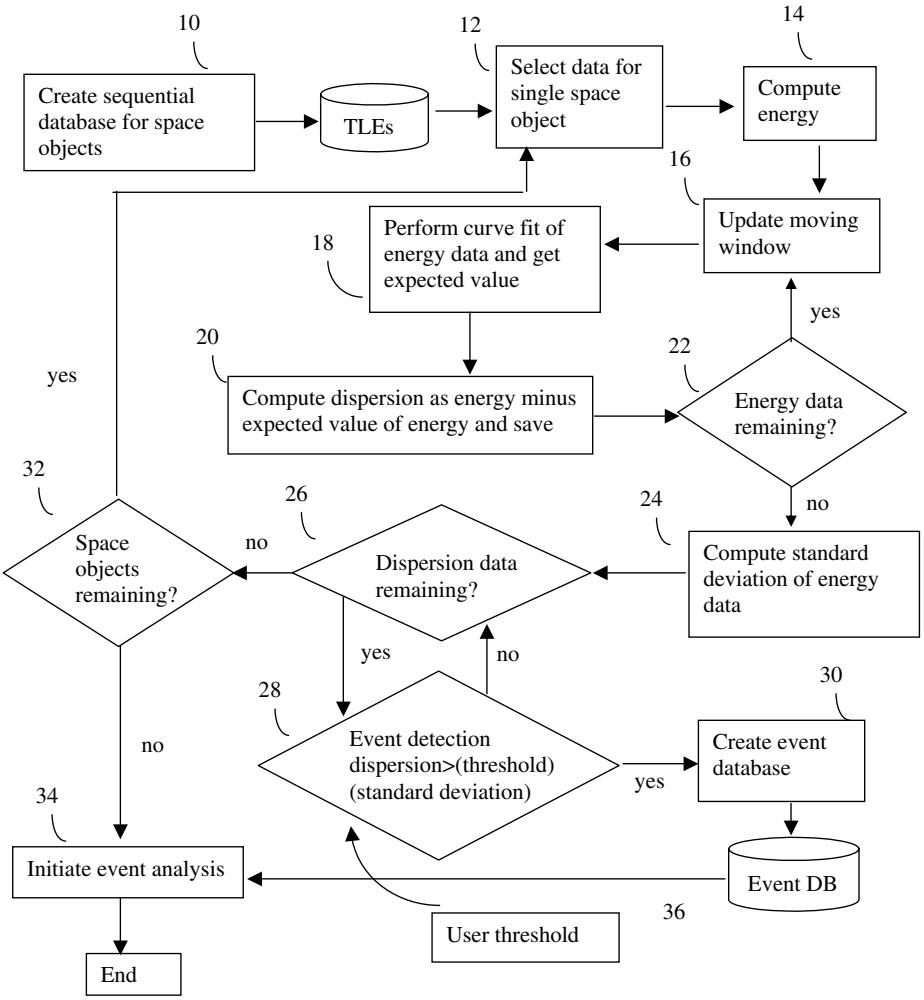

Fig. 1 Processing scheme for energy event detection.

18: The energy data in the moving window are fit to a polynomial function of time. An expected value of energy at the last data time point is computed from the polynomial curve fit.

20: Energy dispersion is computed as the value of energy minus the expected value of energy from the curve fit. The dispersion and associated time are saved in a data array.

22: A check is made to determine if more energy data are available. If so, the moving window is updated by adding the next sequential energy value and removing the oldest energy value. In this manner, the size of the data window does not change, but it moves forward one time value.

24: When no more energy data are available, the standard deviation of the energy dispersions is computed.

26: Each value of dispersion is checked to see if it represents an event. Thus, a check is made to see if a value of dispersion is available for event checking.

28: An event is declared if the dispersion is greater than the standard deviation times a user-supplied threshold. Thus, a threshold value of three corresponds to a three-sigma threshold value.

36: A threshold is supplied by the user. The higher the threshold, the fewer dispersions will exceed the threshold, and the fewer events will be declared.

30: Events are stored in an event database for subsequent processing.

32: A check is made to see if more space objects are available for processing. If so, the next space object with its associated sequential data is selected and the event process begins again. If no more objects are available for processing, the event analysis is begun.

34: Event analysis is initiated for each event in the event database.

36: User defined threshold is used to select the magnitude of event desired.

III. Analysis

Each tracked object has its own file of sequential TLEs spanning the period of interest as illustrated in Fig. 2. Each element set has an associated time and date for the orbital parameters, which include inclination, eccentricity, right ascension of ascending node, argument of perigee, mean anomaly, and mean motion. One can process each individual parameter to detect sudden or unexpected changes, or one can process a parameter that is derived from one or more of the TLE parameters.

Because maneuvers, collisions, and sudden increases in atmospheric density result in changes in energy, energy was considered a very useful parameter for analysis. Energy was computed as kinetic energy plus gravitational energy based on a spherical Earth. Higher order energy terms associated with Earth, moon, and sun were neglected but could be included if desired.

The energy per unit mass was computed from the mean motion n, which is the number of orbits per day traversed by the space object.

$$E = -(0.5)\left[\frac{\pi n G M}{12(60)^2}\right]^{\frac{2}{3}}, \qquad (\mathrm{m/s})^2 \tag{1}$$

where G is the universal gravitational constant and M is the mass of the Earth. Thus, for each TLE time, a value of energy was computed for processing.

The moving window curve fit method, which proved useful in trajectory estimation problems [7], was applied to the space event detection problem. Figure 2 illustrates the moving window curve fit method. The data to be processed are placed in a data array of selected size. For example, the array may contain 12 sequential parameters. A polynomial curve of selected order is fit to the data using the least

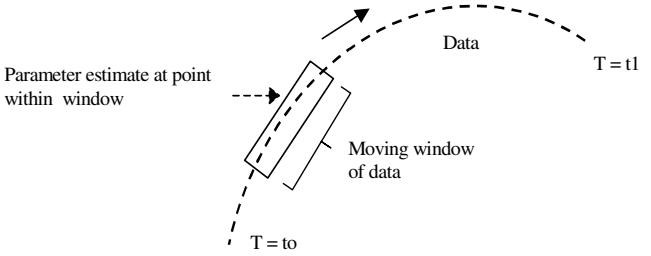

Fig. 2 Moving window curve fit method diagram.

squares method. Time is the independent variable. A parameter value based on the curve fit is computed for a given time within the window. The curve value is subtracted from the actual data at the corresponding time to obtain a dispersion value. The array window is then advanced in time by removing the oldest parameter and adding the next sequential parameter. One could advance the window forward by more than one data set at one time if desired. The number of time steps advanced depends upon the fidelity of the results needed. Once the window is advanced, another curve fit is performed and the resulting deviation is saved. This process is repeated for all of the sequential data.

Equation (2) illustrates a polynomial of order three. The curve fit performs two functions. It filters noise and/or high frequency variation in the data. It also allows parameter or the parameter's time derivative estimation for any time within the window. Increasing the size of the window provides greater filtering of noise. However, larger window sizes require higher order polynomial curve fits to capture the expected variation of the parameter. Thus, there is a trade-off between window size and the order of the curve fit. One can tune the window size and order of the curve fit based on the inherent characteristics of the data. The output of the curve fit is the polynomial coefficients, c_i, illustrated in the Eq. (2). It should be noted that the curve fit is valid only within the window. The curve should not be extrapolated beyond the window,

$$p(t) = c_0 + c_1 t + c_2 t^2 + c_3 t^3 \tag{2}$$

Another method to detect changes in a parameter is to evaluate the derivative of the polynomial curve fit at some time within the window. If a parameter such as energy has a step increase at the midpoint of the window, the derivative of the curve fit would indicate a sharp increase at that point. The derivative simply replaces the parameter dispersion in processing step no. 20 in Fig. 1, and the remainder of the processing scheme remains the same. The derivative of the polynomial curve fit in Eq. (2) is given by

$$\frac{\mathrm{d}p}{\mathrm{d}t} = c_1 + 2c_2 t + 3c_3 t^2 \tag{3}$$

The method can be applied to a historical database or it can process data in real time. In the real time application, the moving window is advanced as new data are received. The processing is essentially the same in both applications.

IV. Event Detection

Events are detected by processing the array of deviations or derivatives that was generated by the moving window processing. In either case, one would like to identify the largest absolute values based on the statistics of the data. The first step is to evaluate the mean of the data by summing the values and dividing by the total number of values summed. Once the average is obtained, the variance and standard deviations are computed based on standard methods. In the real time application, the statistical parameters can be computed recursively rather than in a batch method to increase processing speed.

The data threshold is defined in units of its standard deviation. Once a threshold is selected, each data point is checked to determine if it exceeds the threshold. If a data value exceeds the threshold, an event is declared for that data point. Higher thresholds result in fewer data values exceeding the threshold and fewer events being declared. All data points exceeding the threshold are saved for subsequent processing. Because time is included with each detected event, one can process the initial raw data associated with the event to determine other characteristics of the event.

Other event selection criteria can be used to reduce the number of events or to select the type of event of interest. For example, one could declare an event if two selected parameters exceed their respective thresholds simultaneously. An orbit-raising maneuver would increase energy but not change inclination. However, a random space collision event might change both energy and inclination. Therefore, events involving energy and inclination changes could identify potential collision events. With six orbital parameters to choose from, many other event criteria could be used.

A. Collision Event Detection Example

The first confirmed unintentional random collision in space [8] between two tracked space objects occurred in 1996. Since this collision, which involved the Cerise spacecraft, at least two other collisions between tracked objects have occurred [9]. As an example of this method, TLE data for the object that collided with the Cerise space vehicle were processed using the moving window curve fit method. A window of nine TLEs worth of energy data was fit to a fourth order polynomial, as expressed in step step 18 of Fig. 1. Figure 3 illustrates raw energy data and the polynomial fit to the data for a sample window. The value of energy produced by the curve fit at the end of the window was plotted in Fig. 4. The window was advanced one data point for each cycle. A new curve fit and value of energy was generated and plotted in Fig. 4 for each moving window step. Energy dispersions were saved in a file, as illustrated in step 20 of Fig. 1. The dispersion data were processed to determine the standard deviation (sigma), as expressed in step 24 of Fig. 1. The threshold was set at three-sigma. The event indicator is initially set to

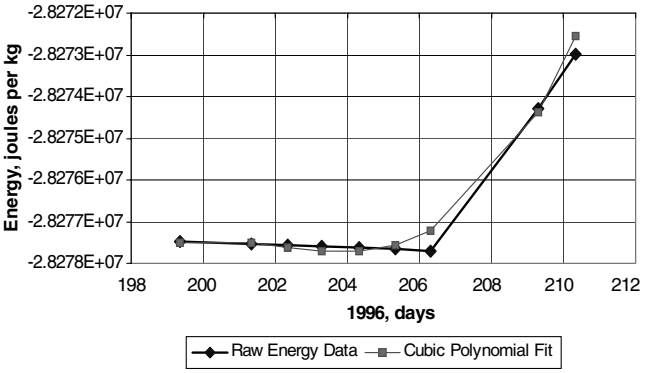

Fig. 3 Sample moving window of energy data for space object no. 18208 that collided with Cerise space vehicle in 1996 and its associated cubic polynomial curve fit.

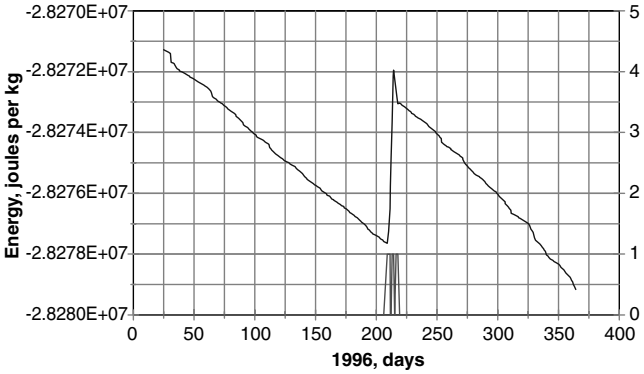

Fig. 4 Energy of space object no. 18208 that collided with Cerise space vehicle in 1996 and the detected event.

zero. Each dispersion is checked to see if it exceeds the threshold. If the threshold is exceeded, the event indicator for the given time step is changed from zero to one, indicating a detected event. This process is repeated for all of the dispersions. This step corresponds to step 28 in Fig. 1. The event indicator is plotted in the lower portion of Fig. 4 to illustrate the time at which each event was detected. Only near day 210 did the energy dispersion exceed three-sigma during the period illustrated in Fig. 4.

Figures 5 and 6 illustrate the associated energy dispersions and derivative, respectively. The event indicator appears at the lower portion of each graph. The up–down variations in the figures are caused by the relative location of the event within the moving window curve fit. As the moving window advances, the event passes through the moving window, which causes variations in the curve fit estimate. Because the moving window contains many TLEs, the effect of a single bad TLE is averaged out and usually does not show up as a detected event. This example demonstrates that the method can successfully detect a space collision event.

A collision event can affect other TLE parameters, as mentioned earlier. An event was also detected by processing inclination data for object no. 18208. Figure 7 illustrates the estimated inclination produced by the moving window curve fit and the events that exceed three-sigma. Only a single event was detected over the time period illustrated in Fig. 7. The event time corresponds to that in Figs. 4–6. Because this event affected both energy and inclination, the event type is likely a collision event. Processing multiple parameters simultaneously may help in determining the type of event detected.

B. Space Weather Event Detection Example

Solar activity can add energetic particles and associated energy to the upper atmosphere and increase its temperature. The hotter atmosphere expands and increases the atmospheric density at higher altitudes. As a result, atmospheric drag increases for objects in low Earth orbit. The change in drag manifests itself in the derived energy dispersion parameter. A large number of tracked space objects had large energy dispersion near day 315 in the year 2004, which indicated a change in drag due to atmospheric density. Figure 8 illustrates the correlation between the dispersion in energy and the Ap index, which is a measure of geomagnetic activity. Evidently, a mass was blown off the solar corona and impacted the Earth's magnetic field triggering the geomagnetic activity and resultant upper atmospheric heating. This event produced changes in upper atmospheric density that affected state vector parameters of object no. 7219. The energy dispersion is observed several days past the event because the event is still within the moving window and therefore influences the curve fit. The solar event illustrated in Fig. 8 was significant enough to affect space objects in orbit having altitudes 1000 km or less.

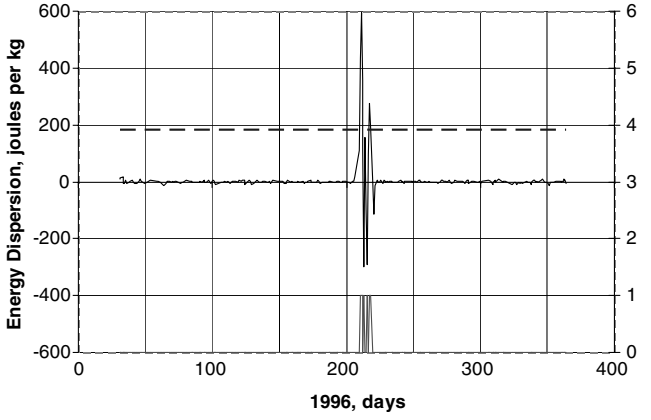

Fig. 5 Energy dispersion of space object no. 18208 that collided with Cerise space vehicle in 1996 with the associated three-sigma threshold. The detected event appears on lower curve.

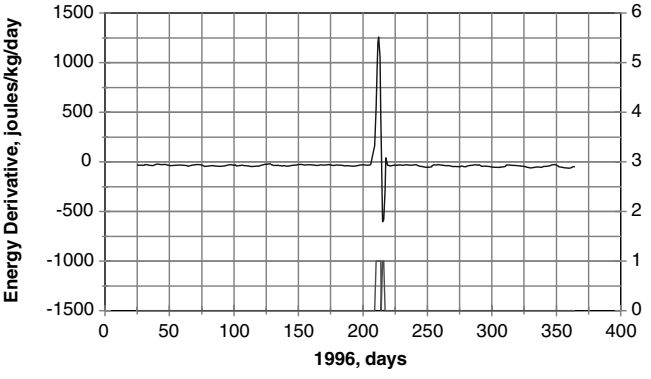

Fig. 6 Energy derivative of space object no. 18208 that collided with Cerise space vehicle in 1996 and the detected event.

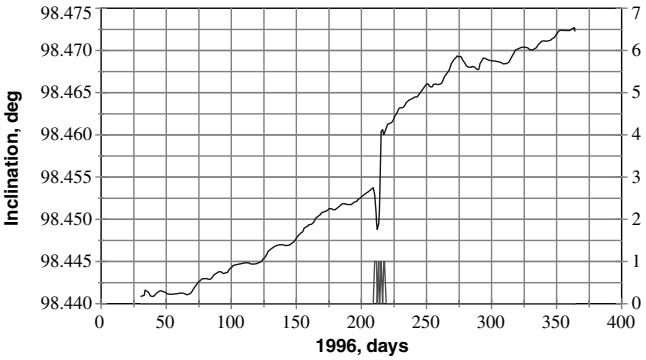

Fig. 7 Inclination of space object no. 18208 that collided with Cerise space vehicle in 1996 and the detected event.

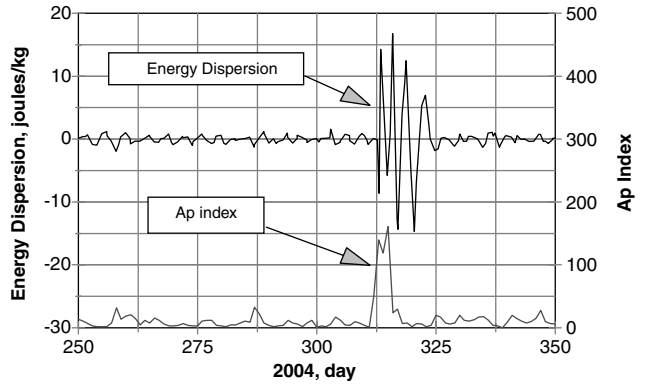

Fig. 8 The dispersion in energy for space object no. 7219 is highly correlated to the Ap index.

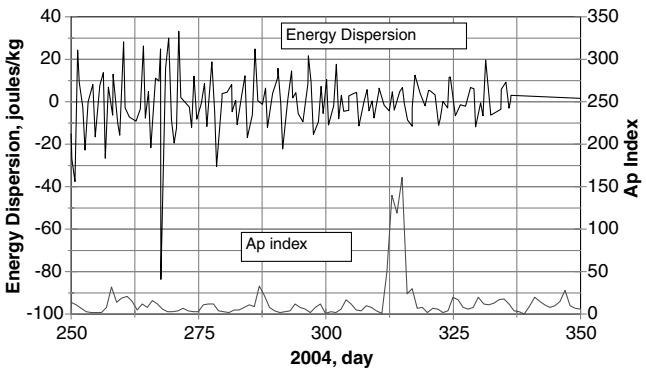

Fig. 9 The dispersion in energy for space object no. 19133 is not correlated to the Ap index.

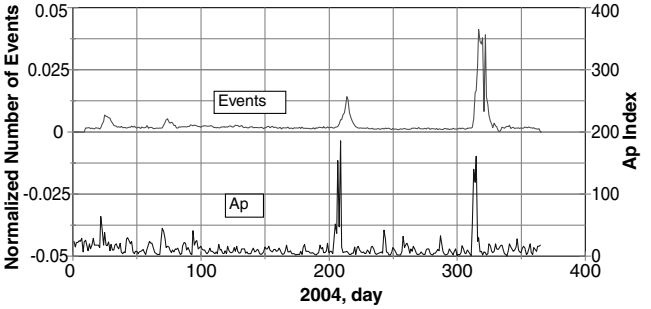

Fig. 10 Normalized number of events per day for the entire unclassified catalog of tracked objects and the Ap index as a function of the day of the year in 2004.

Space objects that orbit above roughly 1000 km are not influenced as much by solar activity as are lower altitude objects. Figure 9 illustrates energy dispersions for space object no. 19133, which has apogee and perigee altitudes of 1594 and 1445 km, respectively. It is clear from the figure that energy dispersions are not correlated to the Ap index because the major increase in the Ap index on day 315 has little or no associated energy dispersion. In this case, the energy dispersion is equal to or less than the inherent error and is not detected as an event.

The catalog of tracked objects was processed to detect space events using the energy parameter. The numbers of events per day for each tracked object were combined to form the total number of events per day for all tracked objects. The normalized number of events per day is found by dividing the number of events per day by the total number of events for the entire year. The normalized number of events per day was plotted versus the day of the year in 2004 as illustrated in Fig. 10.

It took only 2 min and 23 s to process the entire catalog for the entire year of 2004 using a laptop. The processor was an Intel Pentium® M having a speed of 2 GHz and a random access memory of 2 GB.

The two major solar events produce most of the space events. The influence of the solar event on the Ap index persists for a day or two after the event. The correlation between the Ap index and the detected space events is of high interest to both space weather analysts and satellite operators who need accurate state vector information for their vehicle.

Figure 11 illustrates the normalized number of events for space objects having semimajor axes between 1000 and 2000 km for the year 2004. The two major solar events indicated by the spikes in the Ap index do not affect these higher altitude space objects.

It is of interest to determine the range of altitudes of tracked space objects most affected by the elevated Ap index. Detected events for the catalog of tracked space objects were grouped in altitude bins spanning the altitude range between 200 and 1300 km. Event data as a function of the day of the year in 2004 for each altitude bin similar to that in Fig. 10 was generated. The correlation coefficient between the

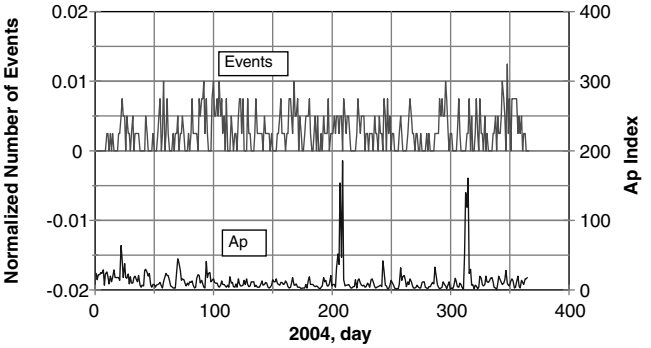

Fig. 11 Normalized number of events per day for the unclassified catalog of tracked objects with semimajor axes between 1000 and 2000 km and the Ap index as a function of the day of the year in 2004.

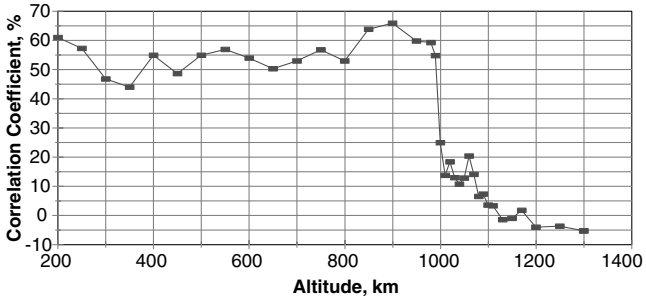

Fig. 12 Correlation between the Ap index and all space events as a function of altitude in 2004.

Ap index as shown in Fig. 10 and the events in each altitude bin were computed and plotted in Fig. 12. One would expect the higher altitude objects to be affected less by the Ap index because they are beyond the reach of even an expanded atmosphere. Calculation of the correlation coefficient supports this expectation because below 1000 km the correlation is in the 45–70% range indicating high correlation. Above 1000 km the correlation coefficient drops well below 10% indicating virtually no correlation. It should be noted that these results are for the year 2004. Future studies will determine if these results can be generalized to other years.

C. Maneuver Detection Example

The space event detection method has the ability to detect space vehicle maneuvers because maneuvers change the vehicle's energy. Even small station keeping maneuvers can be easily detected. Satellites in orbit above about 1000 km are not significantly affected by atmospheric density changes due to solar activity. Gravitational perturbations from the Earth, sun, and moon are extremely small and produce small energy dispersions from the nominal Keplerian energy. As a result, even a very small maneuver stands out as a dominant change in energy. Consequently, satellite maneuvers are easily detected with the proposed processing method. This is because the threshold is proportional to the standard deviation of the dispersions. As the dispersions decrease at higher altitude, so does the event threshold, which enables detection of events with smaller associated energy changes. Figure 13 illustrates maneuver detection for an anonymous space vehicle having an orbital altitude above the range of the Earth's atmosphere. The significant solar event that occurred on day 315 of 2004 is not present in Fig. 13 due to the satellite's high altitude. The threshold was set to three-sigma and several apparent maneuver events were detected. If the threshold were lowered, more events would be detected. However, the threshold should not be lowered too much. For example, a one-sigma threshold could result in more than half the dispersions being detected as events if the dispersions happen to be normally distributed.

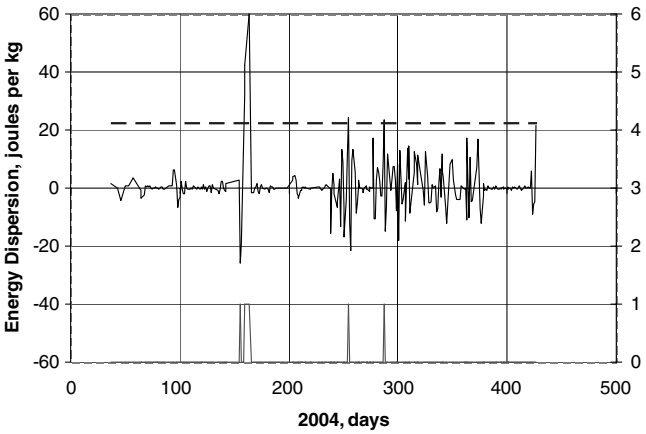

Fig. 13 Energy dispersions and detected events versus day of the year in 2004 for an object that is not affected by atmospheric density fluctuations due to solar activity.

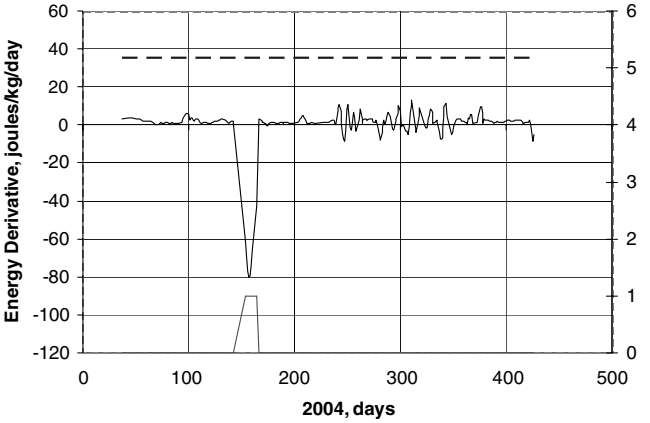

Fig. 14 Energy derivative and detected maneuver event corresponding to Fig. 12.

Figure 14 illustrates the derivative of energy for the same vehicle as in Fig. 13. It is clear that at least one maneuver was made during the period shown. More detailed analysis is required to determine the nature of the smaller oscillations in the derivative appearing in Fig. 14, which may be the result of attitude control maneuvers that inadvertently add or subtract orbital energy.

Figure 15 illustrates the total orbital energy of the International Space Station for the year 2005. The relatively low altitude of its orbit causes a significant orbital decay rate. As a result several orbital boost maneuvers were applied throughout the year. When the event detection threshold was set at three-sigma, three orbital maneuver events were detected. The events corresponded to orbital energy

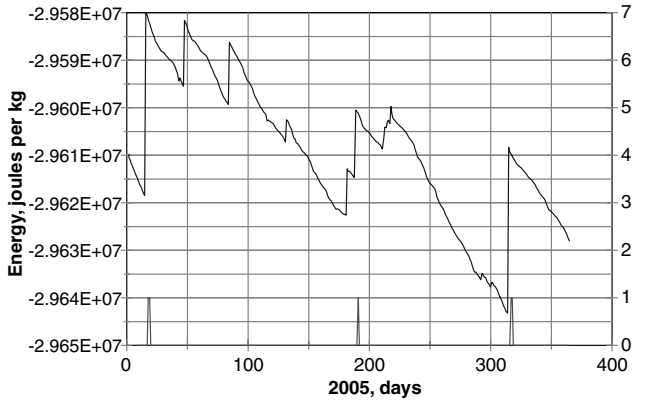

Fig. 15 Energy and detected maneuver events versus day of the year in 2005 for the International Space Station using a three-sigma threshold.

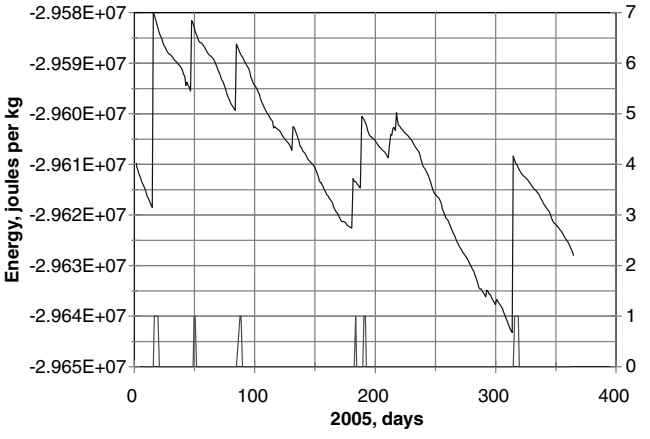

Fig. 16 Energy and detected maneuver events versus day of the year in 2005 for the International Space Station using a two-sigma threshold.

increases as indicated in Fig. 15. When the threshold was set at two-sigma, smaller orbital energy increases were detected as illustrated in Fig. 16. Changes in the orbital energy due to solar activity were significantly smaller than the orbit-raising maneuvers.

This example illustrates that the moving window curve fit method for event detection works well for cases in which the parameter is changing over time. In this case atmospheric drag decreased energy, but the slow change was accommodated by the curve fit method. Only sudden changes in energy associated with the maneuver events were detected.

V. Summary and Conclusions

A data processing method was developed to detect space events including collisions, satellite maneuvers, and solar activity that affect atmospheric density. The method uses state vector data associated with the catalog of tracked objects. The technique can be applied to any element set parameter or a derivative of one or more TLE parameters. Sequential data are processed using a moving window to both filter and estimate a parameter's value. Parameter dispersions are found by differencing its expected value and its actual value. The statistical distribution of the dispersion is used to establish an event threshold. Events are declared when dispersions exceed the event threshold. The method can be used in both batch and recursive modes. The algorithm is very efficient because it took a little more than two minutes to process the entire catalog for an entire year using a laptop computer.

The advantage of the moving window curve fit technique is that only sudden abnormal changes in parameter values are identified. Slower secular parameter variations are accommodated by the method without generating extraneous events.

The method was demonstrated by detecting a space collision event, satellite maneuver events, and events related to solar activity. In each case, dispersions in the energy parameter were used to detect events.

Acknowledgments

The author would like to thank Vladimir Chobotov, John Cox, and Justin McNeill for reviewing this paper and providing many insightful suggestions to improve it.

References

[1] Koons, H. C., and Fennell, J. F., "Space Weather Effects on Communication Satellites," *The Radio Science Bulletin*, Vol. 316, March 2006, pp. 27–41.

[2] Anz-Meador, P. D., and Johnson, N. L., "A Decade of Growth," *Proceedings of the Third European Conference on Space Debris*, ESOC, Darmstadt, Germany, March 2001, pp. 753–758.

[3] Matney, M., Settecerri, T., Johnson, N., and Stansbery, E., "*Characterization of the Breakup of the Pegasus Rocket Body 1994-029B*," *Proceedings of the Second European Conference of Space Debris*, ESOC, Darmstadt, Germany, March 1997, pp. 289–292.

[4] Folcik, Z. J., Cefola, P. J., and Abbot, R. I., "GEO Maneuver Detection for Space Situational Awareness," AAS Paper 07-285, April 2007.

[5] Aaron, B. S., "Geosynchronous Satellite Maneuver Detection and Orbit Recovery Using Ground Based Optical Tracking," Master's Thesis, Massachusetts Institute of Technology, Cambridge, MA, June 2006.

[6] Johnson, N. L., "Activities on Space Debris in U. S.," *Proceedings of the Third European Conference on Space Debris*, ESOC, Darmstadt, Germany, March 2001, pp. 13–19.

[7] Patera, R. P., "Trajectory Estimation Based on Radar Data," *Aerospace Forum on Space Debris, Collision Avoidance, and Reentry Hazards, El Segundo, CA*, The Aerospace Corporation, El Segundo, CA, 1–3 Nov. 2000.

[8] Alby, F., Lansard, E., and Michal, T., "Collision of Cerise with Space Debris," *Proceedings of the Second European Conference on Space Debris, European Space Operations Center*, ESA SP-393,ESA/ESOC, Darmstadt, Germany, March 1997, pp. 589–596.

[9] "Accidental Collisions of Cataloged Satellites Identified," *The Orbital Quarterly News*, NASA, Vol. 9, No. 2, 2005, pp. 1–2.

J. Minow
Associate Editor